



Synthesis and antitumor evaluation of novel hybrids of phenylsulfonylfuroxan and epiandrosterone/dehydroepiandrosterone derivatives



Yaoqing Huang^{a,1}, Mingming Liu^{a,1}, Lanfang Meng^b, Pan Feng^a, Yalan Guo^a, Minghua Ying^c, Xiuyan Zhu^c, Ying Chen^{a,*}

^a Department of Medicinal Chemistry, School of Pharmacy, Fudan University, Shanghai, China

^b Department of Nuclear Medicine, ZhongShan Hospital, Fudan University, Shanghai, China

^c Zhejiang Xianju Pharmaceutical Co. Ltd., Zhejiang, China

ARTICLE INFO

Article history:

Received 20 March 2015
Received in revised form 24 April 2015
Accepted 13 May 2015
Available online 22 May 2015

Keywords:

16,17-Pyrazo-annulated steroids
Furoxan
Cytotoxicity
VEGF inhibitor
Anti-cancer

ABSTRACT

Thirteen novel furoxan-based nitric oxide (NO) releasing hybrids (**14a–e**, **15a–e**, **17b–d**) of 16,17-pyrazo-annulated steroidal derivatives were synthesized and evaluated against the MDA-MB-231, HCC1806, SKOV-3, DU145, and HUVEC cell lines for their in vitro anti-proliferative activity. Most of the compounds displayed potent anti-proliferative effects. Among them, **17c** exhibited the best activity with IC₅₀ values of 20–1.4 nM against four cell lines (MDA-MB-231, SKOV-3, DU145, and HUVEC), and 1.03 μM against a tamoxifen resistant breast cancer cell line (HCC1806). Furthermore, five compounds (**14a**, **15a**, **17b–d**) were selected to screen for VEGF inhibitory activity. Compounds **15a**, **17b,c** showed obviously better activity than 2-Methoxyestradiol (2-ME) on reducing levels of VEGF secreted by MDA-MB-231 cell line. In a Capillary-like Tube Formation Assay, compounds **17b,c** exhibited a significant suppression of the tubule formation in the concentration of 1.75 nM and 58 nM, respectively. The preliminary SAR showed that steroidal scaffolds with a linker in 3-position were favorable moieties to evidently increase the bioactivities of these hybrids. Overall, these results implied that **17c** merited to be further investigated as a promising anti-cancer candidate.

© 2015 Elsevier Inc. All rights reserved.

1. Introduction

Nitric oxide (NO), which is naturally synthesized from L-arginine by the action of NO synthase (NOS), is a key signaling molecule which plays very important roles in diverse physiological and pathophysiological processes including vascular homeostasis maintenance, neurotransmission, and immune response. Nitric oxide diffuses outward and into nearby target cells after being generated, and then all the effects mentioned above are triggered by activating cytosolic guanylate cyclase, thereby stimulating intracellular accumulation of cyclic guanosine monophosphate (cGMP), which acts as an intracellular messenger to initiate a series of reactions [1,2]. It is well-known that high levels of NO can act as a potent anti-cancer agent by promoting apoptosis, inhibiting angiogenesis, and sensitizing tumor cells to chemotherapy, radiation, and immunotherapy [3–6]. High concentration of NO was also

reported to reverse the resistance to doxorubicin in human colon cancer cells [7,8]. Furoxan is an important class of NO donors, which can release high levels of NO in vitro [9]. And their hybrids with other active compounds such as oleanolic acid, glycyrrhetic acid, farnesylthiosalicylic acid, displayed potent antitumor activity both in vitro and in vivo [10–12]. In our prior research, several furoxan-based NO releasing hybrids with the coumarin core were synthesized to exhibit excellent biological activities including antiproliferation of tumor cells, inducing apoptosis of tumor cells and inhibition of angiogenesis [13].

Angiogenesis is dysregulated in many pathological conditions such as cancers. It plays significant roles in tumor growth, invasion and metastasis because of its function for supplying of oxygen, nutrients, growth factors and dissemination of tumor cells to distal sites [14]. Preventing the expansion of new blood vessel networks may result in reduced tumor size and metastases. Vascular endothelial growth factor (VEGF) is the major driver of tumor angiogenesis by triggering endothelial cells to form new capillaries under hypoxic conditions, and high expression of VEGF has been observed in many cancers, including colorectal carcinoma, gastric carcinoma,

* Corresponding author. Tel./fax: +86 21 51980116.

E-mail address: yingchen71@fudan.edu.cn (Y. Chen).

¹ Yaoqing Huang and Mingming Liu are co-first-authors.

pancreatic carcinoma, breast cancer, prostate cancer, lung cancer, and melanoma [14–16]. All these results make VEGF a target for many angiogenesis inhibitors and of keen interest in the field of cancer research [17]. In our prior research, several 16,17-pyrazo-annulated steroids were synthesized and proved to exhibit potent VEGF inhibitory activity. Among them, compound **1** (3 β -O-(3,3-dimethylsuccinyl)-2'-methyl-2'H-androst-16-eno[17,16-c]pyrazole) and **2** (3 β -O-(3,3-dimethylsuccinyl)-2'-phenyl-2'H-androsta-5,16-dieno[17,16-c]pyrazole) exhibited similar EC₅₀ values and obviously better TI values compared with 2-ME [18] (Fig. 1).

It is therefore of interest to develop more desirable leading compounds with steroidal scaffold and explore whether introduction of phenylsulfonylfuroxan moiety to potent antiangiogenesis compounds mentioned above would provide a novel class of NO donating hybrids which may exert positive synergistic antitumor effects. Herein, a series of novel hybrids of phenylsulfonylfuroxan group and 16,17-pyrazo-annulated steroids were designed, synthesized and biologically evaluated for antiproliferation of cancer cell lines, inhibitory activity of VEGF and capillary-like tube formation.

2. Experimental

2.1. General

Melting points were measured on a SGW X-4 microscopy melting point apparatus without correction. ¹H and ¹³C NMR spectral data were recorded with a Varian 400 MHz spectrometer at 303 K using TMS as an internal standard. Mass spectra were recorded on Agilent Technologies 1260 infinity LC/MS instrument, and HRMS spectra were recorded on an Agilent Technologies LC/MSD TOF instrument. Analytical and preparative TLC was performed on silica gel HSGF/UV 254. The chromatograms were conducted on silica gel (100–200 mesh) and visualized under UV light at 254 and 365 nm.

2.2. 3-Phenylsulfonyl-4-hydroxyethoxyl-1,2,5-oxadiazole 2-Oxide (7)

The synthesis of the intermediate **7** from benzenethiol was reported previously in ref [19].

2.3. 3 β -Hydroxy-16-(hydroxymethylene)-5 α -androstan-17-one (10)

Sodium ethoxide (2.12 g, 31.2 mmol) was added to a round-bottomed flask and dissolved in CH₂Cl₂ (40 mL). Then epiandrosterone **8** (0.91 g, 3.12 mmol) and ethyl formate (3.8 mL, 46.8 mmol) were added. The reaction mixture was stirred under nitrogen atmosphere for 5 h at room temperature. Then the solvent was evaporated and water (50 mL) was added. The aqueous phase was acidified with 2 M HCl. Then the precipitated solid was filtered and washed with water. Evaporation of residual water under reduced pressure afforded **10** (0.79 g, 80%) which was sufficiently pure for the next stage. Mp 220–221 °C; ESI-MS *m/z* (%) 319.1 [M+H]⁺; ¹H NMR (400 MHz, CDCl₃) δ 0.73 (s, 3H, H-18), 0.75 (s, 3H, H-19), 4.42 (d, 1H, *J* = 4.31 Hz, H-3), 7.32 (s, 1H, H-1'), 0.61–2.42 (m, 22H).

2.4. 3 β -Hydroxy-16-(hydroxymethylene)androsta-5-en-17-one (11)

11 (0.85 g, 86%) was obtained starting from dehydroepiandrosterone **9** (0.9 g, 3.12 mmol). Mp 238–241 °C; ESI-MS *m/z* (%) 317.2 [M+H]⁺; ¹H NMR (400 MHz, DMSO-*d*₆) δ 1.03 (s, 3H, H-18), 1.09 (s, 3H, H-19), 3.53 (m, 1H, H-3), 5.40 (s, 1H, H-6), 7.16 (s, 1H, H-1'), 1.12–2.59 (m, 19H).

2.5. 2'H-Androst-16-eno[17,16-c]pyrazole-3 β -ol (12a)

Compound **10** (2.00 g, 6.3 mmol) was dissolved in anhydrous ethanol (30 mL), and 85% hydrazine hydrate (1.10 g, 18.8 mmol) was added dropwise to the solution. After being stirred for 0.5 h at room temperature, the mixture was poured into ice water (100 mL). Then the mixture was adjusted to pH 7 by 2 M HCl to afford a white solid. Recrystallization from acetone gave **12a** (1.7 g, 86%). Mp 260–261 °C; ESI-MS *m/z* (%) 315.2 [M+H]⁺; ¹H NMR (400 MHz, CDCl₃) δ 0.87 (s, 3H, H-18), 0.97 (s, 3H, H-19), 3.60 (m, 1H, H-3), 7.14 (s, 1H, —N=CH—), 0.78–2.52 (m, 22H).

2.6. 2'H-Androsta-5,16-dieno[17,16-c]pyrazole-3 β -ol (13a)

13a (1.8 g, 92%) was obtained starting from **11** (2.0 g, 6.3 mmol). Mp 269–272 °C; ESI-MS *m/z* (%) 313.2 [M+H]⁺; ¹H NMR (400 MHz, CDCl₃) δ 1.02 (s, 3H, H-18), 1.08 (s, 3H, H-19), 3.54 (m, 1H, H-3), 5.39 (d, 1H, *J* = 5.16 Hz, H-6), 7.15 (s, 1H, —N=CH—), 1.10–2.56 (m, 19H).

2.7. 2'-methyl-2'H-Androst-16-eno[17,16-c]pyrazole-3 β -ol (12b)

Compound **10** (2.00 g, 6.3 mmol) was dissolved in anhydrous ethanol (30 mL), and 40% methylhydrazine (1.45 g, 12.6 mmol) was added dropwise to the solution. After being stirred for 1 h at room temperature, the mixture was poured into ice water (100 mL). Then the mixture was adjusted to pH 7 by 2 M HCl to afford a white solid. Recrystallization from methanol gave **12b** (1.72 g, 83%). Mp 222–223 °C; ESI-MS *m/z* (%) 329.1 [M+H]⁺; ¹H NMR (400 MHz, CDCl₃) δ 0.86 (s, 3H, H-18), 0.97 (s, 3H, H-19), 3.60 (m, 1H, H-3), 3.81 (s, 3H, —N—CH₃), 6.93 (s, 1H, —N=CH—), 0.79–2.48 (m, 21H).

2.8. 2'-methyl-2'H-Androsta-5,16-dieno[17,16-c]pyrazole-3 β -ol (13b)

13b (1.80 g, 87%) was obtained starting from **11** (2.00 g, 6.3 mmol). Mp 208–210 °C; ESI-MS *m/z* (%) 327.2 [M+H]⁺; ¹H NMR (400 MHz, CDCl₃) δ 1.00 (s, 3H, H-18), 1.07 (s, 3H, H-19), 3.55 (m, 1H, H-3), 3.78 (s, 3H, —N—CH₃), 5.38 (d, 1H, *J* = 4.64 Hz, H-6), 7.12 (s, 1H, —N=CH—), 1.11–2.47 (m, 18H).

2.9. 2'-Phenyl-2'H-androst-16-eno[17,16-c]pyrazole-3 β -ol (12c)

Compound **10** (0.80 g, 2.5 mmol) was dissolved in anhydrous ethanol (20 mL) and phenylhydrazine (0.54 g, 5.0 mmol) was added dropwise to the solution. After being refluxed for 2 h, the mixture was poured into ice water (100 mL). Then the mixture was adjusted to pH 7 by 2 M HCl to afford a light yellow solid. Recrystallization from methanol gave **12c** (0.70 g, 72%). Mp 217–219 °C; ESI-MS *m/z* (%) 391.2 [M+H]⁺; ¹H NMR (400 MHz, CDCl₃) δ 0.84 (s, 3H, H-18), 0.97 (s, 3H, H-19), 3.59 (m, 1H, H-3), 7.32 (t, 1H, *J* = 7.48 Hz, 7.32 Hz, —N—C₆H₅), 7.37 (s, 1H, —N=CH—), 7.42 (t, 2H, *J* = 7.56 Hz, 8.04 Hz, —N—C₆H₅), 7.49 (d, 2H, *J* = 8.0 Hz, —N—C₆H₅), 0.76–2.56 (m, 21H).

2.10. 2'-Phenyl-2'H-androsta-5,16-dieno[17,16-c]pyrazole-3 β -ol (13c)

13c (0.42 g, 86%) was obtained starting from **11** (0.40 g, 1.3 mmol). Mp 232–235 °C; ESI-MS *m/z* (%) 389.0 [M+H]⁺; ¹H NMR (400 MHz, CDCl₃) δ 1.05 (s, 3H, H-18), 1.08 (s, 3H, H-19), 3.53 (m, 1H, H-3), 5.39 (d, 1H, *J* = 5.12 Hz, H-6), 7.32 (t, 1H, *J* = 7.32 Hz, 7.24 Hz, —N—C₆H₅), 7.38 (s, 1H, —N=CH—), 7.42 (t, 2H, *J* = 7.48 Hz, 8.04 Hz, —N—C₆H₅), 7.50 (d, 2H, *J* = 7.60 Hz, —N—C₆H₅), 0.89–2.56 (m, 18H).

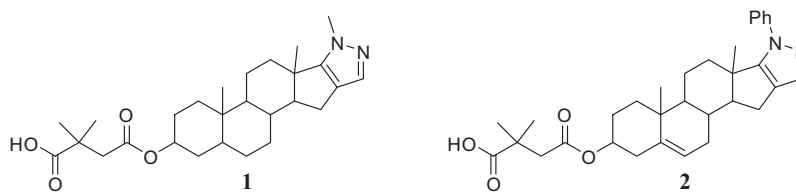


Fig. 1. The structures of compounds **1** and **2**.

2.11. 2'-(1,1-Dimethylethyl)-2'H-androst-16-eno[17,16-c]pyrazole-3 β -ol (**12d**)

Compound **10** (2.00 g, 6.3 mmol) was dissolved in anhydrous ethanol (30 mL) and tert-Butylhydrazine hydrochloride (1.56 g, 12.6 mmol) was added to the solution. After being refluxed for 1 h, the mixture was poured into ice water (100 mL). Then the mixture was adjusted to pH 7 by 2 M NaOH aqueous solution to afford a white solid. Recrystallization from ethyl acetate gave **12d** (1.50 g, 64%). Mp 242–245 °C; ESI-MS m/z (%) 371.2 [M+H]⁺; ¹H NMR (400 MHz, CDCl₃) δ 0.85 (s, 3H, H-18), 1.02 (s, 3H, H-19), 1.60 (s, 9H, $-(CH_3)_3$), 3.61 (m, 1H, H-3), 7.13 (s, 1H, $-N=CH-$), 0.76–2.47 (m, 21H).

2.12. 2'-(1,1-Dimethylethyl)-2'H-androsta-5,16-dieno[17,16-c]pyrazole-3 β -ol (**13d**)

13d (1.85 g, 80%) was obtained starting from **11** (2.00 g, 6.3 mmol). Mp 254–255 °C; ESI-MS m/z (%) 369.2 [M+H]⁺; ¹H NMR (400 MHz, CDCl₃) δ 1.08 (s, 6H, H-18, 19), 1.58 (s, 9H, $-(CH_3)_3$), 3.54 (m, 1H, H-3), 5.40 (d, 1H, $J = 4.64$ Hz, H-6), 7.15 (s, 1H, $-N=CH-$), 1.06–2.50 (m, 18H).

2.13. 3 β -[[5-Oxido-4-(phenylsulfonyl)-1,2,5-oxadiazol-3-yl]oxy]-2'H-androst-16-eno[17,16-c]pyrazole (**14a**) and 2'-[[5-Oxido-4-(phenylsulfonyl)-1,2,5-oxadiazol-3-yl]oxy]-2'H-androst-16-eno[17,16-c]pyrazole-3 β -ol (**14e**)

Compound **12a** (0.20 g, 0.6 mmol) was added to a stirred solution of compound **6** (0.23 g, 0.6 mmol) in the presence of 8-diazabicyclo[5.4.0]undec-7-ene (DBU) (0.19 g, 1.28 mmol) in CH₂Cl₂ (15 mL). The reaction mixture was stirred at room temperature for 3 h and then washed with water (3 \times 30 mL). The organic layer was dried with anhydrous Na₂SO₄. Then the solvent was removed under reduced pressure, and the residue was purified by column chromatography (PE/EtOAc = 10:1–5:1) to yield **14a** (44 mg, 13%) and **14e** (35 mg, 10%) as white solid, respectively.

14a: Mp 128–131 °C; ESI-MS m/z (%) 539.2 [M+H]⁺; ¹H NMR (400 MHz, CDCl₃) δ 0.94 (s, 3H, H-18), 0.99 (s, 3H, H-19), 4.79 (m, 1H, H-3), 7.14 (s, 1H, $-N=CH-$), 7.61 (t, 2H, $J = 7.72$ Hz, 7.48 Hz, $-\text{SO}_2\text{C}_6\text{H}_5$), 7.75 (t, 1H, $J = 7.26$ Hz, 7.48 Hz, $-\text{SO}_2\text{C}_6\text{H}_5$), 8.05 (d, 2H, $J = 8.02$ Hz, $-\text{SO}_2\text{C}_6\text{H}_5$), 0.83–2.55 (m, 21H); ¹³C NMR (101 MHz, CDCl₃) δ 168.42, 158.41, 138.12, 135.52, 129.56, 128.56, 122.83, 121.55, 110.51, 81.95, 62.17, 54.64, 53.44, 44.56, 40.43, 36.40, 35.75, 34.32, 33.94, 33.51, 31.45, 29.67, 28.38, 27.26, 23.91, 20.83, 18.26, 12.30; ESI-HRMS (m/z) [M+H]⁺ Calcd for C₂₈H₃₄N₄O₅S: 539.2323, Found: 539.2327.

14e: Mp 181–184 °C; ESI-MS m/z (%) 539.2 [M+H]⁺; ¹H NMR (400 MHz, CDCl₃) δ 0.90 (s, 3H, H-18), 1.09 (s, 3H, H-19), 3.62 (m, 1H, H-3), 7.60 (t, 2H, $J = 7.92$ Hz, 7.72 Hz, $-\text{SO}_2\text{C}_6\text{H}_5$), 7.65 (s, 1H, $-N=CH-$), 7.75 (t, 1H, $J = 7.36$ Hz, 7.48 Hz, $-\text{SO}_2\text{C}_6\text{H}_5$), 8.18 (d, 2H, $J = 7.64$ Hz, $-\text{SO}_2\text{C}_6\text{H}_5$), 0.85–2.68 (m, 21H); ¹³C NMR (101 MHz, CDCl₃) δ 174.17, 149.20, 137.91, 135.62, 129.37, 129.29, 126.77, 124.52, 113.24, 76.68, 71.13, 61.41, 54.65, 44.85, 40.88, 38.05, 36.79, 35.73, 34.48, 33.61, 31.56, 31.41, 29.67,

28.40, 24.03, 20.74, 18.10, 12.33; ESI-HRMS (m/z) [M+H]⁺ Calcd for C₂₈H₃₄N₄O₅S: 539.2323, Found: 539.2327.

2.14. 3 β -[[5-Oxido-4-(phenylsulfonyl)-1,2,5-oxadiazol-3-yl]oxy]-2'H-androsta-5,16-dieno[17,16-c]pyrazole (**15a**) and 2'-[[5-Oxido-4-(phenylsulfonyl)-1,2,5-oxadiazol-3-yl]oxy]-2'H-androsta-5,16-dieno[17,16-c]pyrazole-3 β -ol (**15e**)

15a (120 mg, 14%) and **15e** (40 mg, 5%) were obtained starting from **13a** (500 mg, 1.6 mmol).

15a: Mp 118–121 °C; ESI-MS m/z (%) 537.2 [M+H]⁺; ¹H NMR (400 MHz, CDCl₃) δ 1.04 (s, 3H, H-18), 1.16 (s, 3H, H-19), 4.71 (m, 1H, H-3), 5.48 (s, 1H, H-6), 7.16 (s, 1H, $-N=CH-$), 7.63 (t, 2H, $J = 7.72$ Hz, 7.68 Hz, $-\text{SO}_2\text{C}_6\text{H}_5$), 7.76 (t, 1H, $J = 7.16$ Hz, 7.20 Hz, $-\text{SO}_2\text{C}_6\text{H}_5$), 8.06 (d, 2H, $J = 8.0$ Hz, $-\text{SO}_2\text{C}_6\text{H}_5$), 0.86–2.60 (m, 18H); ¹³C NMR (101 MHz, CDCl₃) δ 168.50, 158.52, 139.25, 138.34, 135.80, 129.84, 128.85, 123.50, 123.21, 121.91, 110.76, 82.14, 62.48, 50.61, 40.47, 38.03, 37.11, 36.88, 34.06, 32.16, 31.64, 30.40, 27.73, 24.24, 20.75, 19.57, 18.25, 14.38; ESI-HRMS (m/z) [M+H]⁺ Calcd for C₂₈H₃₂N₄O₅S: 537.2166, Found: 537.2167.

15e: Mp 190–193 °C; ESI-MS m/z (%) 537.2 [M+H]⁺; ¹H NMR (400 MHz, CDCl₃) δ 1.11 (s, 3H, H-18), 1.12 (s, 3H, H-19), 3.56 (m, 1H, H-3), 5.40 (s, 1H, H-6), 7.61 (t, 2H, $J = 8.16$ Hz, 7.52 Hz, $-\text{SO}_2\text{C}_6\text{H}_5$), 7.66 (s, 1H, $-N=CH-$), 7.75 (t, 1H, $J = 7.56$ Hz, 7.48 Hz, $-\text{SO}_2\text{C}_6\text{H}_5$), 8.18 (d, 2H, $J = 7.36$ Hz, $-\text{SO}_2\text{C}_6\text{H}_5$), 0.86–2.71 (m, 18H); ¹³C NMR (101 MHz, CDCl₃) δ 174.29, 149.56, 141.34, 138.16, 135.90, 129.65, 126.99, 124.87, 121.21, 113.52, 71.86, 61.79, 50.61, 42.47, 40.91, 37.37, 36.99, 33.81, 32.16, 31.82, 31.55, 30.40, 24.36, 22.94, 20.73, 19.66, 18.10, 14.38; ESI-HRMS (m/z) [M+H]⁺ Calcd for C₂₈H₃₂N₄O₅S: 537.2166, Found: 537.2163.

2.15. 3 β -[[5-Oxido-4-(phenylsulfonyl)-1,2,5-oxadiazol-3-yl]oxy]-2'H-2'-methyl-androst-16-eno[17,16-c]pyrazole (**14b**)

14b (30 mg, 9%) was obtained starting from **12b** (200 mg, 0.6 mmol).

14b: Mp 177–180 °C; ESI-MS m/z (%) 553.2 [M+H]⁺; ¹H NMR (400 MHz, CDCl₃) δ 0.95 (s, 3H, H-18), 0.99 (s, 3H, H-19), 3.80 (s, 3H, $-N-CH_3$), 4.79 (m, 1H, H-3), 7.14 (s, 1H, $-N=CH-$), 7.61 (t, 2H, $J = 8.04$ Hz, 7.72 Hz, $-\text{SO}_2\text{C}_6\text{H}_5$), 7.76 (t, 1H, $J = 7.48$ Hz, 7.56 Hz, $-\text{SO}_2\text{C}_6\text{H}_5$), 8.06 (d, 2H, $J = 7.32$ Hz, $-\text{SO}_2\text{C}_6\text{H}_5$), 0.84–2.49 (m, 20H); ¹³C NMR (101 MHz, CDCl₃) δ 158.61, 157.47, 138.35, 135.78, 133.94, 129.81, 128.84, 124.01, 110.77, 82.02, 62.73, 54.61, 44.90, 41.64, 36.99, 36.60, 36.00, 34.29, 34.11, 33.76, 31.53, 29.94, 28.52, 27.42, 24.53, 20.91, 17.60, 12.57; ESI-HRMS (m/z) [M+Na]⁺ Calcd for C₂₉H₃₆N₄O₅S: 575.2299, Found: 575.2295.

2.16. 3 β -[[5-Oxido-4-(phenylsulfonyl)-1,2,5-oxadiazol-3-yl]oxy]-2'H-2-phenyl-androst-16-eno[17,16-c]pyrazole (**14c**)

14c (40 mg, 12%) was obtained starting from **12c** (200 mg, 0.5 mmol).

14c: Mp 247–248 °C; ESI-MS m/z (%) 615.2 [M+H]⁺; ¹H NMR (400 MHz, CDCl₃) δ 0.93 (s, 3H, H-18), 1.05 (s, 3H, H-19), 4.78 (m, 1H, H-3), 7.32 (t, 1H, $J = 7.24$ Hz, 7.32 Hz, $-\text{N}-\text{C}_6\text{H}_5$), 7.37 (s, 1H, $-\text{N}=\text{CH}-$), 7.42 (t, 2H, $J = 7.48$ Hz, 8.12 Hz, $-\text{N}-\text{C}_6\text{H}_5$), 7.49 (d, 2H, $J = 7.36$ Hz, $-\text{N}-\text{C}_6\text{H}_5$), 7.62 (t, 2H, $J = 8.12$ Hz, 7.60 Hz, $-\text{SO}_2\text{C}_6\text{H}_5$), 7.75 (t, 1H, $J = 7.40$ Hz, 7.52 Hz, $-\text{SO}_2\text{C}_6\text{H}_5$), 8.06 (d, 2H, $J = 7.28$ Hz, $-\text{SO}_2\text{C}_6\text{H}_5$), 0.82–2.57 (m, 20H); ¹³C NMR (101 MHz, CDCl₃) δ 158.34, 156.98, 140.47, 138.09, 135.49, 135.20, 129.54, 128.86, 128.56, 127.11, 126.09, 123.47, 110.50, 81.77, 62.84, 54.21, 44.60, 42.63, 36.28, 35.66, 34.90, 34.19, 33.49, 31.28, 29.67, 28.27, 27.13, 24.08, 20.69, 17.76, 12.27; ESI-HRMS (m/z) [M+H]⁺ Calcd for C₃₄H₃₈N₄O₅S: 615.2636, Found: 615.2631.

2.17. 3β-[[5-Oxido-4-(phenylsulfonyl)-1,2,5-oxadiazol-3-yl]oxy]-2'H-2'-(1,1-dimethylethyl)-androsta-5,16-dieno[17,16-c]pyrazole (**14d**)

14d (100 mg, 13%) was obtained starting from **12d** (0.5 g, 1.35 mmol).

14d: Mp 222–224 °C; ESI-MS m/z (%) 595.2 [M+H]⁺; ¹H NMR (400 MHz, CDCl₃) δ 0.95 (s, 3H, H-18), 1.04 (s, 3H, H-19), 1.58 (s, 9H, $-(\text{CH}_3)_3$), 4.80 (m, 1H, H-3), 7.14 (s, 1H, $-\text{N}=\text{CH}-$), 7.62 (t, 2H, $J = 8.04$ Hz, 7.76 Hz, $-\text{SO}_2\text{C}_6\text{H}_5$), 7.76 (t, 1H, $J = 7.52$ Hz, 7.48 Hz, $-\text{SO}_2\text{C}_6\text{H}_5$), 8.06 (d, 2H, $J = 7.40$ Hz, $-\text{SO}_2\text{C}_6\text{H}_5$), 0.83–2.48 (m, 20H); ¹³C NMR (101 MHz, CDCl₃) δ 158.35, 155.65, 138.10, 135.50, 131.13, 129.54, 128.57, 126.03, 110.50, 81.81, 62.81, 58.85, 53.92, 44.55, 43.72, 36.88, 36.31, 35.59, 34.38, 33.46, 31.25, 30.64, 28.32, 27.14, 23.60, 21.14, 17.36, 12.26; ESI-HRMS (m/z) [M+H]⁺ Calcd for C₃₂H₄₂N₄O₅S: 595.2949, Found: 595.2950.

2.18. 3β-[[5-Oxido-4-(phenylsulfonyl)-1,2,5-oxadiazol-3-yl]oxy]-2'H-2'-methyl-androsta-5,16-dieno[17,16-c]pyrazole (**15b**)

15b (50 mg, 7%) was obtained starting from **13b** (400 mg, 1.2 mmol).

15b: Mp 192–193 °C; ESI-MS m/z (%) 551.2 [M+H]⁺; ¹H NMR (400 MHz, CDCl₃) δ 1.02 (s, 3H, H-18), 1.14 (s, 3H, H-19), 3.79 (s, 3H, $-\text{N}-\text{CH}_3$), 4.71 (m, 1H, H-3), 5.46 (s, 1H, H-6), 7.12 (s, 1H, $-\text{N}=\text{CH}-$), 7.62 (t, 2H, $J = 8.0$ Hz, 7.68 Hz, $-\text{SO}_2\text{C}_6\text{H}_5$), 7.76 (t, 1H, $J = 7.56$ Hz, 7.48 Hz, $-\text{SO}_2\text{C}_6\text{H}_5$), 8.06 (d, 2H, $J = 7.44$ Hz, $-\text{SO}_2\text{C}_6\text{H}_5$), 0.85–2.64 (m, 17H); ¹³C NMR (101 MHz, CDCl₃) δ 158.25, 158.81, 138.83, 138.07, 135.54, 133.05, 129.56, 128.59, 123.26, 110.50, 81.78, 62.55, 50.16, 41.03, 37.73, 36.79, 36.58, 33.84, 31.90, 31.41, 31.15, 30.13, 27.41, 24.31, 22.67, 20.31, 19.26, 17.10, 14.12; ESI-HRMS (m/z) [M+H]⁺ Calcd for C₂₉H₃₄N₄O₅S: 551.2323, Found: 551.2317.

2.19. 3β-[[5-Oxido-4-(phenylsulfonyl)-1,2,5-oxadiazol-3-yl]oxy]-2'H-2'-phenyl-androsta-5,16-dieno[17,16-c]pyrazole (**15c**)

15c (10 mg, 13%) was obtained starting from **13c** (50 mg, 0.13 mmol).

15c: Mp 237–239 °C; ESI-MS m/z (%) 613.2 [M+H]⁺; ¹H NMR (400 MHz, CDCl₃) δ 1.10 (s, 3H, H-18), 1.12 (s, 3H, H-19), 4.70 (m, 1H, H-3), 5.47 (s, 1H, H-6), 7.33 (t, 1H, $J = 7.16$ Hz, 7.36 Hz, $-\text{N}-\text{C}_6\text{H}_5$), 7.39 (s, 1H, $-\text{N}=\text{CH}-$), 7.43 (t, 2H, $J = 7.48$ Hz, 8.04 Hz, $-\text{N}-\text{C}_6\text{H}_5$), 7.50 (d, 2H, $J = 7.44$ Hz, $-\text{N}-\text{C}_6\text{H}_5$), 7.62 (t, 2H, $J = 7.88$ Hz, 7.84 Hz, $-\text{SO}_2\text{C}_6\text{H}_5$), 7.76 (t, 1H, $J = 7.48$ Hz, 7.44 Hz, $-\text{SO}_2\text{C}_6\text{H}_5$), 8.06 (d, 2H, $J = 7.36$ Hz, $-\text{SO}_2\text{C}_6\text{H}_5$), 0.88–2.60 (m, 17H); ¹³C NMR (101 MHz, CDCl₃) δ 158.24, 156.86, 140.46, 138.86, 138.06, 135.63, 135.20, 129.56, 128.89, 128.59, 127.14, 126.09, 123.47, 123.21, 110.49, 81.77, 62.94, 49.95, 42.36, 37.72, 36.73, 36.52, 34.71, 31.17, 30.61, 29.67, 27.38, 24.13, 20.35, 19.23, 17.56; ESI-HRMS (m/z) [M+H]⁺ Calcd for C₃₄H₃₆N₄O₅S: 613.2479, Found: 613.2476.

2.20. 3β-[[5-Oxido-4-(phenylsulfonyl)-1,2,5-oxadiazol-3-yl]oxy]-2'H-2'-(1,1-dimethylethyl)-androsta-5,16-dieno[17,16-c]pyrazole (**15d**)

15d (52 mg, 17%) was obtained starting from **13d** (188 mg, 0.54 mmol).

15d: Mp 219–222 °C; ESI-MS m/z (%) 593.2 [M+H]⁺; ¹H NMR (400 MHz, CDCl₃) δ 1.08 (s, 3H, H-18), 1.14 (s, 3H, H-19), 1.59 (s, 9H, $-(\text{CH}_3)_3$), 4.71 (m, 1H, H-3), 5.48 (s, 1H, H-6), 7.15 (s, 1H, $-\text{N}=\text{CH}-$), 7.63 (t, 2H, $J = 7.80$ Hz, 7.96 Hz, $-\text{SO}_2\text{C}_6\text{H}_5$), 7.76 (t, 1H, $J = 7.36$ Hz, 7.56 Hz, $-\text{SO}_2\text{C}_6\text{H}_5$), 8.07 (d, 2H, $J = 8.36$ Hz, $-\text{SO}_2\text{C}_6\text{H}_5$), 0.87–2.60 (m, 17H); ¹³C NMR (101 MHz, CDCl₃) δ 158.51, 156.19, 139.02, 138.33, 135.81, 131.16, 129.84, 128.85, 126.37, 123.57, 110.76, 82.05, 63.10, 59.56, 49.94, 43.88, 37.96, 36.95, 36.80, 31.43, 31.12, 30.91, 27.66, 23.92, 21.10, 19.50, 17.45; ESI-HRMS (m/z) [M+H]⁺ Calcd for C₃₂H₄₀N₄O₅S: 593.2792, Found: 593.2787.

2.21. 3β-O-succinyl-2'H-2'-methyl-androsta-5,16-dieno[17,16-c]pyrazole (**16b**)

Compound **13b** (0.35 g, 1.1 mmol), succinic anhydride (0.69 g, 5.4 mmol) and DMAP (0.13 g, 1.1 mmol) were dissolved in anhydrous Py (20 mL). After being refluxed for 4 h, the mixture was poured into ice water (100 mL). The mixture was adjusted to pH 3 by 2 M HCl to afford a brown solid. The crude product was purified by column chromatography (PE/EtOAc = 5:1) to yield **16b** (0.35 g, 77%).

16b: Mp 225–231 °C; ESI-MS m/z (%) 427.2 [M+H]⁺; ¹H NMR (400 MHz, CDCl₃) δ 1.05 (s, 3H, H-18), 1.08 (s, 3H, H-19), 2.62 (m, 4H, $-\text{COCH}_2\text{CH}_2\text{CO}-$), 3.92 (s, 3H, $-\text{N}-\text{CH}_3$), 4.63 (m, 1H, H-3), 5.39 (d, 1H, $J = 4.20$ Hz, H-6), 7.01 (s, 1H, $-\text{N}=\text{CH}-$), 1.58–2.39 (m, 18H).

2.22. 3β-O-succinyl-2'H-2'-phenyl-androsta-5,16-dieno[17,16-c]pyrazole (**16c**)

16c (1.07 g, 85%) was obtained starting from **13c** (1.00 g, 2.6 mmol).

16c: Mp 222–226 °C; ESI-MS m/z (%) 489.8 [M+H]⁺; ¹H NMR (400 MHz, CDCl₃) δ 1.06 (s, 3H, H-18), 1.08 (s, 3H, H-19), 2.62 (m, 4H, $-\text{COCH}_2\text{CH}_2\text{CO}-$), 4.63 (m, 1H, H-3), 5.42 (s, 1H, H-6), 7.33 (t, 1H, $J = 7.16$ Hz, 7.40 Hz, $-\text{N}-\text{C}_6\text{H}_5$), 7.40 (s, 1H, $-\text{N}=\text{CH}-$), 7.43 (t, 2H, $J = 7.44$ Hz, 8.08 Hz, $-\text{N}-\text{C}_6\text{H}_5$), 7.50 (d, 2H, $J = 7.56$ Hz, $-\text{N}-\text{C}_6\text{H}_5$), 0.83–2.67 (m, 18H).

2.23. 3β-O-succinyl-2'H-2'-(1,1-dimethylethyl)-androsta-5,16-dieno[17,16-c]pyrazole (**16d**)

16d (0.40 g, 90%) was obtained starting from **13d** (0.35 g, 0.95 mmol).

16d: Mp 253–256 °C; ESI-MS m/z (%) 469.2 [M+H]⁺; ¹H NMR (400 MHz, CDCl₃) δ 1.07 (s, 3H, H-18), 1.12 (s, 3H, H-19), 1.72 (s, 9H, $-\text{C}(\text{CH}_3)_3$), 2.63 (m, 4H, $-\text{COCH}_2\text{CH}_2\text{CO}-$), 4.62 (m, 1H, H-3), 5.41 (s, 1H, H-6), 7.54 (s, 1H, $-\text{N}=\text{CH}-$), 1.56–2.42 (m, 18H).

2.24. 3β-[[4-[[5-Oxido-4-(phenylsulfonyl)-1,2,5-oxadiazol-3-yl]oxy]ethoxy-4-oxobutanoyl]oxy]-2'H-2'-methyl-androsta-5,16-dieno[17,16-c]pyrazole (**17b**)

DMAP (50 mg, 0.42 mmol) and compound **7** (100 mg, 0.35 mmol) were added to a mixture solution of compound **16b** (150 mg, 0.35 mmol) and DCC (90 mg, 0.42 mmol) in CH₂Cl₂ (15 mL). The reaction mixture was stirred at room temperature for 24 h. Filtration and removal of the solvent in vacuo afforded the crude product, which was subsequently purified by column chromatography using (PE/EtOAc = 5:1) to give **17b** (110 mg, 45%).

17b: Mp 62–64 °C; ESI-MS m/z (%) 695.2 [M+H]⁺; ¹H NMR (400 MHz, CDCl₃) δ 1.01 (s, 3H, H-18), 1.08 (s, 3H, H-19), 2.67 (m, 4H, —COCH₂CH₂CO—), 3.83 (s, 3H, —N—CH₃), 4.53–4.64 (m, 5H, H-3, —furoxan—OCH₂CH₂), 5.40 (s, 1H, H-6), 6.95 (s, 1H, —N=CH—), 7.63 (t, 2H, $J = 7.52$ Hz, 7.80 Hz, —SO₂C₆H₅), 7.76 (t, 1H, $J = 7.24$ Hz, 7.40 Hz, —SO₂C₆H₅), 8.07 (d, 2H, $J = 7.84$ Hz, —SO₂C₆H₅), 0.86–2.55 (m, 17H); ¹³C NMR (101 MHz, CDCl₃) δ 172.13, 171.53, 168.93, 158.69, 139.93, 138.06, 135.66, 129.69, 128.65, 124.28, 122.26, 121.95, 110.41, 74.40, 68.87, 62.12, 61.39, 50.51, 40.47, 38.61, 38.09, 36.88, 36.86, 34.01, 31.46, 30.79, 29.70, 29.31, 29.02, 27.73, 24.29, 20.56, 19.29, 18.17; ESI-HRMS (m/z) [M+Na]⁺ Calcd for C₃₅H₄₂N₄O₉S: 717.2565, Found: 717.2580.

2.25. 3β-[[4-[[5-Oxido-4-(phenylsulfonyl)-1,2,5-oxadiazol-3-yl]oxy]ethanoxy-4-oxobutanoyl]oxy]-2'H-2'-phenyl-androsta-5,16-dieno[17,16-c]pyrazole (**17c**)

17c (124 mg, 53%) was obtained starting from **16c** (150 mg, 0.31 mmol) and **7** (80 mg, 0.30 mmol).

17c: Mp 103–106 °C; ESI-MS m/z (%) 757.4 [M+H]⁺; ¹H NMR (400 MHz, CDCl₃) δ 1.05 (s, 3H, H-18), 1.08 (s, 3H, H-19), 2.66 (m, 4H, —COCH₂CH₂CO—), 4.51–4.64 (m, 5H, H-3, —furoxan—OCH₂CH₂), 5.41 (s, 1H, H-6), 7.33 (t, 1H, $J = 7.32$ Hz, 7.28 Hz, —N—C₆H₅), 7.38 (s, 1H, —N=CH—), 7.43 (t, 2H, $J = 7.52$ Hz, 8.12 Hz, —N—C₆H₅), 7.50 (d, 2H, $J = 7.44$ Hz, —N—C₆H₅), 7.63 (t, 2H, $J = 8.04$ Hz, 7.68 Hz, —SO₂C₆H₅), 7.76 (t, 1H, $J = 7.52$ Hz, 7.48 Hz, —SO₂C₆H₅), 8.07 (d, 2H, $J = 7.36$ Hz, —SO₂C₆H₅), 0.86–2.58 (m, 17H); ¹³C NMR (101 MHz, CDCl₃) δ 172.39, 171.79, 158.90, 157.62, 140.18, 140.00, 138.21, 135.92, 135.02, 129.94, 129.23, 128.88, 127.73, 126.40, 123.89, 122.39, 110.64, 74.50, 69.09, 63.19, 61.62, 50.23, 42.71, 38.23, 36.96, 34.90, 31.40, 30.91, 29.94, 29.50, 29.22, 27.87, 24.42, 20.55, 19.46, 17.82; ESI-HRMS (m/z) [M+H]⁺ Calcd for C₄₀H₄₄N₄O₉S: 757.2902, Found: 757.2919.

2.26. 3β-[[4-[[5-Oxido-4-(phenylsulfonyl)-1,2,5-oxadiazol-3-yl]oxy]ethanoxy-4-oxobutanoyl]oxy]-2'H-2'-(1,1-dimethylethyl)-androsta-5,16-dieno[17,16-c]pyrazole (**17d**)

17d (117 mg, 50%) was obtained starting from **16d** (150 mg, 0.32 mmol) and **7** (920 mg, 0.32 mmol).

17d: Mp 154–156 °C; ESI-MS m/z (%) 737.2 [M+H]⁺; ¹H NMR (400 MHz, CDCl₃) δ 1.06 (s, 6H, H-18,19), 1.59 (s, 9H, —C(CH₃)₃), 2.67 (m, 4H, —COCH₂CH₂CO—), 4.52–4.64 (m, 5H, H-3, —furoxan—OCH₂CH₂), 5.41 (s, 1H, H-6), 7.17 (s, 1H, —N=CH—), 7.63 (t, 2H, $J = 8.0$ Hz, 7.64 Hz, —SO₂C₆H₅), 7.76 (t, 1H, $J = 7.56$ Hz, 7.44 Hz, —SO₂C₆H₅), 8.07 (d, 2H, $J = 7.48$ Hz, —SO₂C₆H₅), 1.06–2.50 (m, 17H); ¹³C NMR (101 MHz, CDCl₃) δ 172.13, 171.53, 158.69, 155.71, 139.68, 138.06, 135.66, 131.16, 129.70, 128.65, 126.12, 122.35, 110.42, 74.33, 68.87, 63.00, 61.39, 58.93, 49.83, 49.13, 43.54, 38.00, 36.83, 36.78, 36.72, 33.95, 31.93, 31.23, 30.95, 30.68, 29.70, 29.31, 29.02, 27.68, 25.63, 24.95, 23.69, 20.86, 19.22, 17.32; ESI-HRMS (m/z) [M+Na]⁺ Calcd for C₃₈H₄₈N₄O₉S: 759.3034, Found: 759.3053.

2.27. 3β-[[4-(2-Hydroxyl-ethanoxy)-4-oxobutanoyl]oxy]-2'H-2'-phenyl-androsta-5,16-dieno[17,16-c]pyrazole (**18c**)

Compound **16c** (3.50 g, 7.2 mmol) was dissolved in anhydrous CH₂Cl₂ (40 mL). Oxalyl chloride (2.45 mL, 25.2 mmol) was added dropwise at 0 °C to a stirred solution. After being stirred for 3 h, ethylene glycol (7.5 mL, 132.2 mmol) was added dropwise to the solution. After being stirred for 3 h, water (5 mL) was added to quench the reaction. Then the mixture was washed with water (3 × 20 mL). The organic layer was dried with anhydrous Na₂SO₄.

The solvent was removed under reduced pressure and the residue was purified by column chromatography (CH₂Cl₂/MeOH = 50:1) to yield **18c** (0.5 g, 13%) as a white solid.

18c: Mp 195–198 °C; ESI-MS m/z (%) 533.4 [M+H]⁺; ¹H NMR (400 MHz, CDCl₃) δ 1.06 (s, 3H, H-18), 1.08 (s, 3H, H-19), 2.65 (m, 4H, —COCH₂CH₂CO—), 3.68 (t, 2H, $J = 5.84$ Hz, 5.64 Hz, HOCH₂—), 4.35 (t, 2H, $J = 5.60$ Hz, 5.84 Hz, HOCH₂CH₂COO—), 4.63 (m, 1H, H-3), 5.42 (d, 1H, $J = 4.84$ Hz, H-6), 7.32 (t, 1H, $J = 7.40$ Hz, 7.24 Hz, —N—C₆H₅), 7.38 (s, 1H, —N=CH—), 7.42 (t, 2H, $J = 7.52$ Hz, 8.0 Hz, —N—C₆H₅), 7.50 (d, 2H, $J = 7.84$ Hz, —N—C₆H₅), 1.06–2.59 (m, 18H); ¹³C NMR (101 MHz, CDCl₃) δ 172.58, 171.91, 157.03, 140.53, 139.79, 135.19, 128.89, 127.17, 126.16, 123.57, 122.23, 74.35, 66.33, 63.04, 61.11, 50.10, 42.43, 38.02, 36.77, 34.83, 31.21, 30.74, 29.61, 27.66, 24.18, 20.38, 19.22, 17.57; ESI-HRMS (m/z) [M+H]⁺ Calcd for C₃₂H₄₀N₂O₅: 533.3010, Found: 533.3014.

2.28. In vitro antiproliferative assay

The in vitro antiproliferation of the chemical compounds was measured by the MTT reagent. Briefly, 5 × 10³ cells in 100 μL of medium per well were plated in 96-well plates. After being incubated for 24 h, the cells were treated with different concentration of tested compound or DMSO (as negative control) for 48 h. Then the medium with compound or DMSO was replaced with 200 μL of fresh medium containing 10% MTT (5 mg/mL in PBS) in each well and incubated at 37 °C for 4 h. Last, the MTT-containing medium was discarded and 150 μL of DMSO per well was added to dissolve the formazan crystals newly formed. Absorbance of each well was determined by a microplate reader (Synergy H4, Bio-Tek) at a 570 nm wavelength. The inhibition rates of proliferation were calculated with the following equation:

$$\text{Inhibition ratio (\%)} = (\text{OD}_{\text{DMSO}} - \text{OD}_{\text{compd}}) / (\text{OD}_{\text{DMSO}} - \text{OD}_{\text{blank}}) \times 100$$

The concentrations of the compounds that inhibited cell growth by 50% (IC₅₀) were calculated using GraphPad Prism, version 6.0.

2.29. VEGF bioactivity detection

The single human breast cancer cell MDA-MB-231 suspension in 1640 medium with 10% foetal bovine serum at a concentration of 5 × 10³ cells in 100 μL of medium per well were plated in 96-well plates. After incubated for 24 h, the cells were treated with different concentration of tested compound or DMSO (as negative control) at 37 °C with 5% CO₂ for 48 h. The IC₅₀ was obtained by the MTT assay as described before. Conditioned medium from each sample was then collected and stored at –20 °C. The VEGF inhibitory rate was detected using VEGF ELISA kit (R & D Systems, Minneapolis, MN). The EC₅₀ was obtained by calculation from the diagram of inhibitory rate vs. sample concentration.

2.30. Capillary-like tube formation assay

Capillary-like tube formation assay was performed by following the procedure published previously. Briefly, 70 μL per well Matrigel (Corning, NY) was added to 96-well plates and incubated at 37 °C for 30 min to allow gelation to occur. HUVECs were added to the top of the gel at a density of 3 × 10⁴ cells/well in the presence of tested compound or vehicle control (DMSO). Cells were incubated at 37 °C with 5% CO₂ overnight, and pictures were captured with a CCD Sencicam camera mounted on a Olympus inverted microscope.

3. Results

3.1. Chemistry

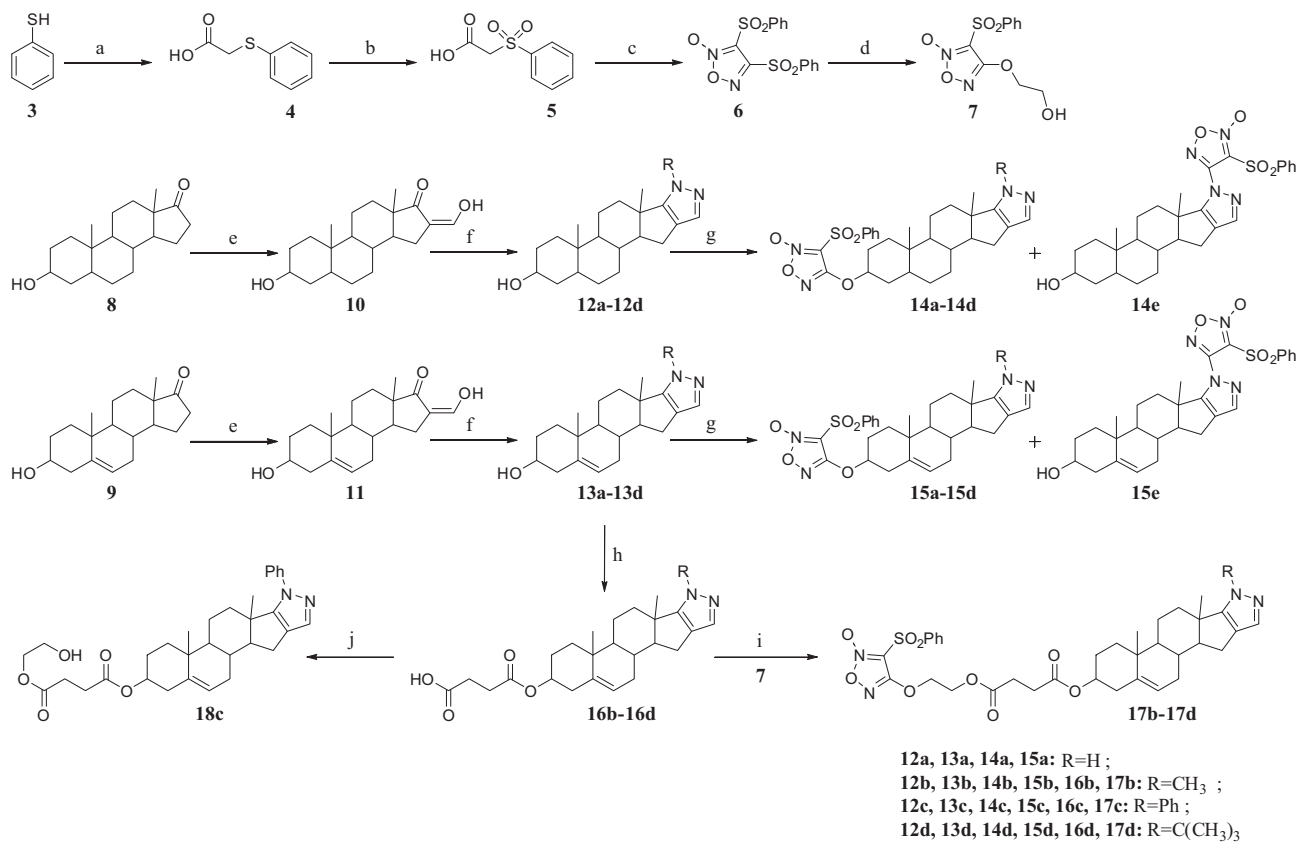
Using epiandrosterone **8** and dehydroepiandrosterone **9** as the starting materials, via C-16 formylation, condensation with mono-substituted hydrazines, esterification of C-3 hydroxyl group with succinic anhydride, and coupling with phenylsulfonyl-substituted furoxan, thirteen different 16,17-pyrazo-annulated steroidal derivatives were synthesized.

As Scheme 1 depicted, phenylsulfonyl-substituted furoxans **6** and **7** were synthesized as described previously. Commercial available compounds **8** and **9** were reacted with ethyl formate to give 16-formylepiandrosterone (**10**) and 16-formyldehydroepiandrosterone (**11**), respectively. Compound **10** was treated with different monosubstituted hydrazines to give compounds **12a–d** in 64–86% yield. Compounds **13a–d** were prepared in the same way from compound **11** in 80–92% yield. Then phenylsulfonyl-substituted furoxan **6** was introduced into compounds **12a–d** and **13a–d** in the presence of 8-diazabicyclo[5.4.0]undec-7-ene (DBU) to give target compounds **14a–d**, **15a–d** and two byproducts (**14e**, **15e**), respectively. Furthermore, the mixture of the compounds **13b–d**, succinic anhydride and catalytic amount 4-N,N-dimethylaminopyridine (DMAP) were refluxed in dry pyridine to give compounds **16b–d** in 77–90% yield, which esterified with **7** in the presence of dicyclohexylcarbodiimide (DCC)/DMAP to generate compounds **17b–d** in 45–53% yield. The compound **18c** was synthesized via the esterification of **16c** with ethylene glycol in the CH₂Cl₂ solution containing oxalyl chloride.

3.2. Biological evaluations

The thirteen newly synthesized hybrids (**14a–e**, **15a–e**, **17b–d**) were evaluated for their cytotoxic effects against the following five cell lines: MDA-MB-231 (human breast cancer cell line), HCC1806 (tamoxifen resistant human breast cancer cell line), SKOV-3 (human ovary cancer cell line), DU145 (human prostate cancer cell line), and HUVEC (umbilical vein endothelium cell line). As shown in Table 1, most target compounds displayed better anti-proliferative activity than that of control compound phenylsulfonylfuroxan **6** (IC₅₀ values of 0.65–2.97 μM). Seven of them (**14a,b**, **15a,b**, **17b–d**) had significant anti-proliferative effects with the IC₅₀ values of 0.0014–0.34 μM against MDA-MB-231, 0.0034–0.70 μM against SKOV-3, 0.02–0.36 μM against DU145, and had considerable cytotoxicity for the tamoxifen resistant cancer cell line HCC1806 in 1.03–2.22 μM values. Among them, compounds **17b–d** exhibited activities in the nanomolar range. In particular, compound **17c** was the most potent molecule. It not only inhibited the proliferation of MDA-MB-231, SKOV-3 and DU145 with IC₅₀ values of 1.4, 3.4, and 20.0 nM, respectively, but also had a strong cytotoxicity for the drug resistance cell line HCC1806 with IC₅₀ value of 1.03 μM.

Moreover, angiogenesis is necessary for tumor growth and metastasis, which makes it a promising target for cancer treatment. Human umbilical vein endothelial cells (HUVECs) are normal cells useful for assessing antiangiogenic potential [14]. HUVEC was also screened in company with the previous four cancer cell lines. Ten of the thirteen compounds showed potent activity with IC₅₀ values less than 1 μM. Compounds **17b,d** demonstrated activity against HUVEC with IC₅₀ of 0.12 and 0.05 μM, respectively. Compound **17c**



Scheme 1. Synthetic routes of target compounds^a. ^aReagents and conditions: (a) ClCH₂COOH, NaOH (aq.), 140 °C, 2 h; (b) 30% H₂O₂, AcOH, r.t., 3.5 h; (c) fuming HNO₃, 90 °C, 4 h; (d) Ethanediol, 25% NaOH (aq.), r.t., 1 h; (e) ethyl formate, C₂H₅ONa, CH₂Cl₂, r.t.; (f) NH₂NHR, C₂H₅OH, r.t. or reflux; (g) furoxan **6**, DBU, CH₂Cl₂, r.t.; (h) succinic anhydride, DMAP, Py, reflux; (i) DCC, DMAP, CH₂Cl₂, r.t.; (j) (COCl)₂, 0 °C, ethanediol, pyridine, r.t.

Table 1
Antiproliferation activities of **14a–e**, **15a–e**, **17b–d**.

Compound	MDA-MB-231 (IC ₅₀ , μM) ^a	HCC1806 (IC ₅₀ , μM) ^a	SKOV-3 (IC ₅₀ , μM) ^a	DU145 (IC ₅₀ , μM) ^a	HUVEC (IC ₅₀ , μM) ^a
14a	0.16	1.82	0.40	0.11	0.03
14b	0.34	2.04	0.70	0.36	0.26
14c	12.36	>60	20.35	15.73	6.79
14d	2.39	20.11	3.88	2.46	1.60
14e	1.04	1.97	0.89	1.08	0.42
15a	0.28	2.22	0.61	0.22	0.17
15b	0.26	1.71	0.50	0.25	0.17
15c	2.43	>60	6.72	2.47	1.47
15d	1.03	19.55	2.31	1.22	0.66
15e	1.32	2.46	1.58	1.37	0.49
17b	0.09	1.80	0.19	0.18	0.12
17c	0.0014	1.03	0.0034	0.02	0.0035
17d	0.04	1.34	0.15	0.10	0.05
Furoxan (6)	1.62	2.97	2.25	0.65	1.42

^a The data are the mean of triplicate determinations; IC₅₀ is the concentration of sample for 50% cell growth inhibitory rate.

Table 2
VEGF inhibitory activities of **14a**, **15a**, **17b–d**.

Compound	IC ₅₀ (μM) ^a	VEGF EC ₅₀ (μM) ^a	TI (IC ₅₀ /EC ₅₀) ^b
14a	0.16	0.06	2.67
15a	0.28	0.04	7.00
17b	0.09	0.01	9.00
17c	0.0014	0.0003	4.67
17d	0.04	0.01	4.00
18c	6.78	2.71	2.50
Furoxan (6)	1.62	1.47	1.10
2-ME	0.25	0.07	3.57

^a The data are the mean of triplicate determinations.

^b EC₅₀ is the concentration of sample for 50% VEGF inhibitory rate; IC₅₀ is the concentration of sample for 50% cell growth inhibitory rate; TI (therapeutic index) = IC₅₀/EC₅₀.

exhibited the highest potency with an IC₅₀ value of 3.5 nM in the assay. The results implied that these new compounds might also be active on angiogenesis targets like vascular endothelial growth factor (VEGF) or its receptor (VEGFR) and encouraged us to further explore their pharmacological mechanism in the following work.

Therefore, five compounds (**14a**, **15a**, **17b–d**) possessing better activity were selected to test for VEGF inhibitory activity in MDA-MB-231 using 2-Methoxyestradiol (2-ME) and furoxan **6** as references. As shown in Table 2, three compounds (**15a**, **17b,c**) effectively reduced the secretion of VEGF in MDA-MB-231 with the EC₅₀ values of 40, 10 and 0.3 nM, respectively, and also exhibited obviously better TI (IC₅₀/EC₅₀) values of 7.00, 9.00 and 4.67 compared with 2-ME (TI = 3.57) and furoxan (TI = 1.10). Meanwhile, in order to confirm whether phenylsulfonylfuroxan moiety played an important role in these novel compounds on VEGF inhibitory activity, compound **18c** was also synthesized as a control which indeed showed worse activity with the EC₅₀ value of 2.71 μM and the TI value of 2.50 than that of the hybrids. These results elucidated that the hybrids of 16,17-pyrazo-annulated steroidal derivatives and furoxan were more favorable than the individuals in inhibiting the secretion of VEGF.

Furthermore, based on the above preliminary results of VEGF inhibitory activity, compounds **17b,c** were selected to perform capillary-like tube formation assay to investigate their inhibition of angiogenesis in vitro with Sunitinib as a positive control. As displayed in Fig. 2, HUVEC cells formed a complete network structure overnight with serum stimulation. Then the tubule formation was slightly suppressed in a concentration of 23 nM (1/5 IC₅₀) of **17b** and 0.7 nM (1/5 IC₅₀) of **17c**. And **17b** with the concentration of 58 nM (1/2 IC₅₀) and **17c** with 1.75 nM (1/2 IC₅₀) almost disrupted the formation of tube structures. All above phenomena suggested that the anti-angiogenesis mechanism of these derivatives of steroidal scaffold coupling with furoxan might be related to the inhibition of secretion of VEGF.

According to the results mentioned above, the preliminary structure–activity relationship (SAR) of the hybrids can be inferred. First, the modification at the 20-position with H, methyl, phenyl and tertiary butyl showed that the smaller group such as hydrogen atom and methyl substitution (**14a,b**, **15a,b**) were more favorable for anti-proliferation activity. Meanwhile, the coupling site of 16,17-pyrazo-annulated steroidal skeleton with furoxan had a slight impact on the cytotoxic potency of the derivatives. The compounds **14a** and **15a** obtained by coupling phenylsulfonylfuroxan to the 3-OH of the steroidal skeleton were more active than the two byproducts **14e** and **15e** obtained by coupling furoxan to the 20-position. Second, the linker between steroidal skeleton and

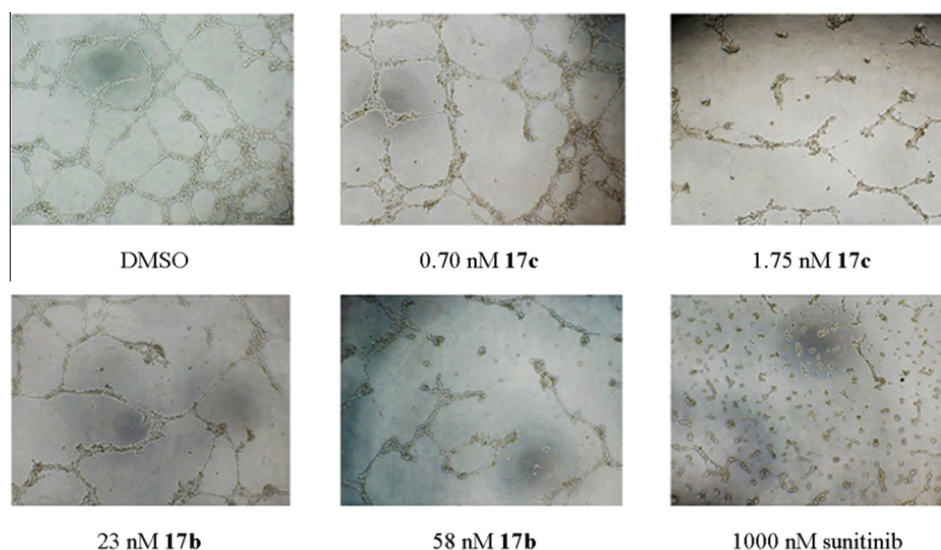


Fig. 2. Capillary-like tube formation assay. (A) Tube formation for the vehicle control. HUVECs formed robust tube structures when they were only treated with vehicle (DMSO). (B) Tubule formation was slightly suppressed with 0.70 nM **17c** treatment. (C) Tubule formation was significantly suppressed with 1.75 nM **17c** treatment. (D) Tubule formation was slightly suppressed with 23 nM **17b** treatment. (E) Tubule formation was significantly suppressed with 58 nM **17b** treatment. (F) Sunitinib was used as a positive control.

furoxan was crucial to preserve the strong anticancer activity. For example, **17b–d** with a linker in 3-position showed stronger anti-proliferation activities against all four tested cancer cell lines than **15b–d**, respectively. The activities of compound **17c** bearing the phenyl in the 20-position were enhanced from 60 to 1900 fold than that of **15c** without a linker at 3-position. The results also implied that with or without double bond in the 5-position of androsterone core had little influence on their activities. However, the structure–activity relationship of the substituent group in the 20-position seemed uncertain: in those target compounds **14a–d** and **15a–d** without the linker, hydrogen atom and smaller size group like methyl located at the 20-position were more beneficial to keep the better potent activities, whereas in the hybrids **17b–d** containing the linker, larger group size like phenyl substituted at 20-position was observed to have the better anti-cancer activity. However, the precise SAR of these hybrids and the optimal compound **17c** with potent anti-tumor activity remain to be further investigated.

4. Conclusions

In summary, thirteen novel furoxan-based nitric oxide (NO) releasing hybrids (**14a–e**, **15a–e**, **17b–d**) of 16, 17-pyrazo-annulated steroidal derivatives were prepared and tested for their in vitro anti-cancer activity. Most of the compounds showed strong anti-proliferative effects better than that of furoxan toward MDA-MB-231, SKOV-3, DU145 and HUVEC cell lines, and even nine of them exhibited considerable cytotoxicity against a tamoxifen resistant human breast cancer cell line HCC1806. Compound **17c** had the best activity against the five cell lines mentioned above. In the preliminary pharmacological study, compounds **15a**, **17b,c** showed obviously better activities compared with 2-ME on reducing levels of VEGF secreted by MDA-MB-231. Besides, **17b,c** significantly suppressed tubule formation at the concentration of nanomolar level. The initial SAR indicated that the linker between furoxan group and steroidal scaffold was very important to notably improve their anti-tumor potency. Further investigation of structure–activity relationship and structure optimization should be conducted in the future. In summary, all above results prompted that compound **17c** might be a desirable candidate for further development.

Acknowledgements

This study was supported by grants from the Shanghai Natural Science Foundation (Grant 14ZR1401900 for Y.C.), China Postdoctoral Science Foundation (Grant 2013M531126 for M.-M.L.).

References

- [1] Ignarro LJ. Signal transduction mechanisms involving nitric oxide. *Biochem Pharmacol* 1991;41:485–90.
- [2] Gasco A, Fruttero R, Sorba G, Stilo AD, Calvino R. NO donors: focus on furoxan derivatives. *Pure Appl Chem* 2004;76:973–81.
- [3] Ridnour LA, Thomas DD, Switzer C, Flores-Santana F, Isenberg JS, Ambs S, Roberts DD, Wink DA. Molecular mechanisms for discrete nitric oxide levels in cancer. *Nitric Oxide* 2008;19:73–6.
- [4] Coulter JA, McCarthy HO, Xiang J, Roedel W, Wagner E, Robson T, Hirst DG. Nitric oxide—a novel therapeutic for cancer. *Nitric Oxide* 2008;19:192–8.
- [5] Bonavida B, Baritaki S, Huerta-Yepez S, Vega MI, Chatterjee D, Yeung K. Novel therapeutic applications of nitric oxide donors in cancer: roles in chemo- and immunosensitization to apoptosis and inhibition of metastases. *Nitric Oxide* 2008;19:152–7.
- [6] Sullivan R, Graham CH. Chemosensitization of cancer by nitric oxide. *Curr Pharm Des* 2008;14:1113–23.
- [7] Riganti C, Miraglia E, Viariso D, Costamagna C, Pescarmona G, Ghigo D, Bosia A. Nitric oxide reverts the resistance to doxorubicin in human colon cancer cells by inhibiting the drug efflux. *Cancer Res* 2005;65:516–25.
- [8] Chegaev K, Riganti C, Lazzarato L, Rolando B, Guglielmo S, Campia I, et al. Nitric oxide donor doxorubicins accumulate into doxorubicin-resistant human colon cancer cells inducing cytotoxicity. *ACS Med Chem Lett* 2011;2:494–7.
- [9] Aguirre G, Boiani M, Cerecetto H, Fernández M, González M, León E, Pintos C, Raymondo S, et al. Furoxan derivatives as cytotoxic agents: preliminary in vivo antitumoral activity studies. *Pharmazie* 2006;61:54–9.
- [10] Lai Y, Shen L, Zhang Z, Liu W, Zhang Y, Ji H, Tian J. Synthesis and biological evaluation of furoxan-based nitric oxidoreleasing derivatives of glycyrrhetic acid as anti-hepatocellular carcinoma agents. *Bioorg Med Chem Lett* 2010;20:6416–20.
- [11] Ling Y, Ye X, Zhang Z, Zhang Y, Lai Y, Ji H, Peng S, Tian J. Novel nitric oxide-releasing derivatives of farnesylthiosalicylic acid: synthesis and evaluation of antihepatocellular carcinoma activity. *J Med Chem* 2011;54:3251–9.
- [12] Chen L, Zhang Y, Kong X, Lan E, Huang Z, Peng S, Kaufman DL, Tian J. Design, synthesis, and antihepatocellular carcinoma activity of nitric oxide releasing derivatives of oleoic acid. *J Med Chem* 2008;51:4834–8.
- [13] Liu MM, Chen XY, Huang YQ, Feng P, Guo YL, Yang G, Chen Y. *J Med Chem* 2014;57:9343–56.
- [14] Hicklin DJ, Ellis LM. Role of the vascular endothelial growth factor pathway in tumor growth and angiogenesis. *J Clin Oncol* 2005;23:1011–27.
- [15] Fayette J, Soria JC, Armand JP. Use of angiogenesis inhibitors in tumour treatment. *Eur J Cancer* 2005;41:1109–16.
- [16] Siejka A, Barabutis N, Schally AV. GHRH antagonist inhibits focal adhesion kinase (FAK) and decreases expression of vascular endothelial growth factor (VEGF) in human lung cancer cells in vitro. *Peptides* 2012;37:63–8.
- [17] Ishak RS, Aad SA, Kyei A, Farhat FS. Cutaneous manifestations of anti-angiogenic therapy in oncology: Review with focus on VEGF inhibitors. *Crit Rev Oncol Hemat* 2014;90:152–64.
- [18] Liu HS, Zheng HL, Ge M, Xia P, Chen Y. Synthesis and VEGF inhibitory activity of 16, 17-pyrazo-annulated steroids. *Chinese Chem Lett* 2011;22:757–60.
- [19] Chen L, Qiu W, Tang J, Wang ZF, He SY. Synthesis and bioactivity of novel nitric oxide-releasing ursolic acid derivatives. *Chin Chem Lett* 2011;22:413–6.